

Analysis of CO₂ Pressure Swing Adsorption Simulation by Considering the Transport Phenomena in the Adsorber

Takehiro Esaki^{1*}, Hideaki Kuronuma², Noriyuki Kobayashi²

¹Department of Chemical Engineering, Faculty of Engineering, Fukuoka University, Fukuoka, Japan

²Chemical systems engineering, Graduate School of Engineering, Nagoya University, Aichi, Japan

Email: *tesaki@fukuoka-u.ac.jp

How to cite this paper: Esaki, T., Kuronuma, H. and Kobayashi, N. (2021) Analysis of CO₂ Pressure Swing Adsorption Simulation by Considering the Transport Phenomena in the Adsorber. *Journal of Materials Science and Chemical Engineering*, 9, 39-54.

<https://doi.org/10.4236/msce.2021.93004>

Received: October 23, 2020

Accepted: March 28, 2021

Published: March 31, 2021

Copyright © 2021 by author(s) and Scientific Research Publishing Inc. This work is licensed under the Creative Commons Attribution International License (CC BY 4.0).

<http://creativecommons.org/licenses/by/4.0/>



Open Access

Abstract

This study focused on CO₂ separation technology with adsorption. This paper describes the analysis carried out by a CO₂ pressure swing adsorption simulation to scale up the absorber. An unsteady one-dimensional balance model was constructed by considering the material, energy, and momentum. In the CO₂ breakthrough test, the beginning time and CO₂ concentration at outlet of CO₂ breakthrough in the calculation were almost equivalent to that of experiment results. The correlation consistency of the calculation results with the analysis model and the experimental results obtained by a bench scale experiment was evaluated. The transport phenomena in the adsorber were investigated at the adsorption, rinse, and desorption steps according to the calculation results. The starting time of CO₂ breakthrough obtained by the analysis is equal to that obtained by the adsorption breakthrough experiment. This confirms that the CO₂ adsorption, and the temperature and velocity distribution in the adsorber, change as a function of the adsorption, rinse, and desorption steps, respectively. Additionally, the CO₂ concentration of the captured gas and the amount of CO₂ quantity were 93.4% per day and 2.9 ton/day, respectively. These values are equal to those obtained by the bench scale experiment.

Keywords

Carbon Dioxide Separation, Pressure Swing Adsorption, Numerical Analysis

1. Introduction

Currently, global warming is considered as a global problem, and various global warming prevention measures are being developed. Carbon dioxide (CO₂) is

produced by the burning of fossil fuels and released into the atmosphere. Notably, CO₂ accounts for the largest portion of discharged greenhouse gases. Therefore, the establishment of the Carbon Capture Storage process (CCS), which comprises CO₂ discharge restraint technology and CO₂ separation and capture technology, is desired to achieve high energy efficiency and establish processes for controlling, capturing, and storing the CO₂ discharged by industrial processes. The CO₂ percentage in the exhausted gas volume has been reported to be approximately 10% - 20%. Hence, it is necessary to separate CO₂ using the CCS process and collect pure CO₂ in the high state [1]. In the CCS process, the energy cost for CO₂ separation is large. Amine absorption, physical absorption, pressure swing adsorption (PSA), film separation, and low-temperature processing are considered in separation technology. Particularly, PSA is a separation technology that uses an adsorbent whereby CO₂ is attached or removed by introducing an exhaust into the adsorption tower to prioritize the absorption of CO₂. The pressure inside the tower is decompressed in a pulsometer after adhesion balance and the CO₂ is collected.

With regard to the CO₂ adhesion pill, substantial development and proposals have been contributed by previous studies on CO₂ separation and collection technology using the PSA method (for example, Kodama *et al.*, 2013) [2]. Additionally, the improvement of the CO₂ separation performance by PSA driving has been reported. Li *et al.* (2009) removed the water vapor from activated alumina, selected CO₂ as a route for separating the adhesion in zeolite 13X, and ensured the promoting effect of the CO₂ adhesion separation.

The CO₂ dissociation has practical use at large-scale facilities (1000 - 10,000 ton/day) and takes place inside the shaft furnace used in steel ironwork and recovery plants. Therefore, it is assumed that the scale of the adsorption tower, wherein the adhesion pill is filled, is also large. When driving for scale-up to expand the adsorption tower, it is necessary to understand the migration phenomenon in the adsorption tower and consider it in the design to achieve a high CO₂ collection rate. In this study, the behavior inside the adsorption tower was considered in the modal PSA using numerical analysis to scale up the CO₂ adsorption tower.

Choi *et al.* (2003) [3] investigated absorption and washing, and obtained the optimal value of the driving condition by experiment and analysis with consideration to laboratory-scale PSA, which assumes the selection of an exhausting process and considers the temperature change in the adsorption tower and the consistency between the experimental and analysis results. Anshul (2010) [4] performed a check in the tower while driving, and used numerical analysis to achieve a high CO₂ collection density.

Many PSA analyses have been reported, but only few analyses have focused on the momentum of the introduced gas. When using the CO₂ separation and recovery technique, the CO₂ amount is high at the gas stream entrance. Particularly, depending on the adhesion operation at the exit, the CO₂ gas volume de-

creases. The pressure fluctuation caused by the change in the adsorption and desorption is large because it becomes a batch wise process later in the modal PSA. Additionally, the momentum of the CO₂ gas depends on the phenomena of adsorption and desorption, and disappears and appears accordingly. Therefore, it is assumed to influence the adsorption and desorption. In this study, a non-regular simultaneous equation that considers the mass, energy, and momentum was established, and an analysis model was developed. To establish each equation, the required physical properties were obtained from the literature, while unclear values were obtained by experiment.

We confirmed that the verification of analysis model by comparing to the experimental CO₂ breakthrough result. The beginning time of breakthrough to the adsorber and CO₂ concentration at outlet adsorber time variation was evaluated in the experiment and calculation. The calculation result obtained by the analysis model was larger than the experimental result for the adsorption tower obtained in the bench scale experiment; therefore, the consistency of the model was confirmed. The CO₂ in the tower and the temperature and flow distribution were considered by the numerical value more than the calculation result. Additionally, the phenomena inside the PSA adsorption tower were elucidated and the PSA driving was estimated.

2. Transport Phenomena in Adsorber

2.1. Pressure Swing Adsorption Step

Figure 1 and **Table 1** present the process of the PSA method considered in this study. The exhaust including CO₂ circulates gas inside the adsorption tower during the adsorption in the elevated pressure process from an art process, and CO₂ adheres to the adhesion pill. After the adhesion balance, the fluid is changed and the process shifts to the washing process. The purge process converts impurities into a dense fog and supplies CO₂ gas to the adsorption tower. The supplied CO₂ has a high degree of purity, owing to the washing process, and remains in the tower where it is decompressed during the decompression attachment and removal process. Finally, CO₂ with high attached or removed purity is collected. The adsorption in the elevated pressure, washing, and decompression attachment and removal processes assumes that the driving is successively switched over for one of the adsorption towers in the PSA method.

The phenomena in the adsorption tower caused by each process occurring in the tower are considered. The adsorption tower specifications were established by an analysis model as presented in **Table 2**. The equipment shape of the adsorption tower imitates the ASCOA-3 adsorption tower of JFE Engineering Corp. Considering the corrosive nature of the dense fog, and the condensation by which the gas inflowing into the CO₂ adsorption tower is SO_x and NO_x, we assume that gaseous H₂O is removed. The adhesion pill uses ZEORAM F-9 obtained from Sumitomo Seika Chemicals Co., Ltd., which is a NaX-type zeolite and can be uniformly filled into the adsorption tower.

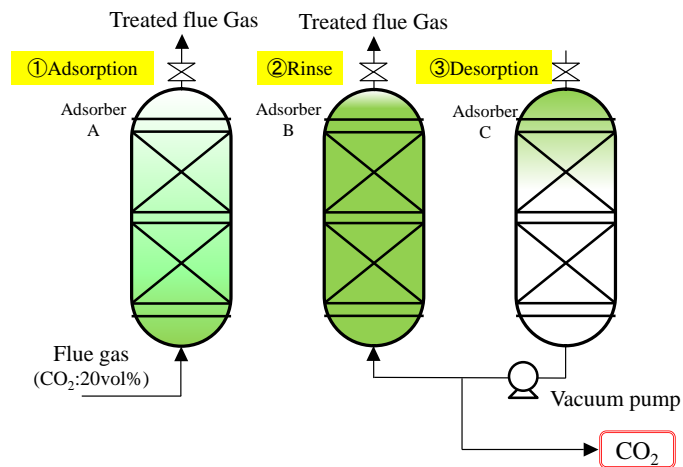


Figure 1. PSA cycle operation (STEP1).

Table 1. State of adsorbers in each step of PSA operation.

	Adsorber A	Adsorber B	Adsorber C
STEP1	Adsorption	Rinse	Desorption
STEP2	Rinse	Desorption	Adsorption
STEP3	Desorption	Adsorption	Rinse

Table 2. Adsorber specifications.

Adsorbent weight [kg]	300
Adsorber height [m]	1.06
Adsorber diameter [m]	0.75

2.2. Analysis Model

The phenomenon of substance migration in the adsorption tower, the energy, and momentum were modeled for each ingredient, and an income and expenditure system was built. The model target is a pillar-like adsorption tower. The analysis model is a one-dimensional non-stationary model that solves the income and expenditure problem in a coalesced manner. The adsorption tower is divided and its minute volume is set to one cell. Additionally, we assumed that the movement is formed by the gradient between the cell and its neighbors. The diffusion, advective, and adhesion items are considered, and the heat conduction of the adhesion pill, advective term, and adhesion heat are also considered by the heat energy income and expenditure in the material balance. The viscosity, advective term, adhesion, and pressure loss are considered in the momentum balance. The CO₂ performs advection by the gas stream between the adsorbent particles. When only CO₂ spreads in the pore, advection is performed for the adsorbent particles. The condition of the adsorption tower entrance and exit are different in each process. Therefore, the boundary conditions switch over when each process reaches the change time. The solution is a positive solution and uses the Crank-Nicholson method. The established income and expenditure

system was scatterized and analyzed using a program developed in the C programming language.

The income and expenditure process and the subjunctive condition of the analysis model are discussed below.

The material balance system in the adsorber is expressed as follows:

$$\frac{\partial \rho_i}{\partial t} = D_{\text{bulk},i} \frac{\partial^2 \rho_i}{\partial z^2} - \frac{\partial(u \rho_i)}{\partial z} - \rho_{\text{bulk}} \frac{\partial q}{\partial t} \quad (1)$$

The heat energy balance system in the adsorber is expressed as follows:

$$\begin{aligned} & \left\{ \varepsilon_{\text{bulk}} \rho_{\text{gas}} C_{p\text{-gas}} + (1 - \varepsilon_{\text{bulk}}) \rho_{\text{Ads}} C_{p\text{-Ads}} \right\} \frac{\partial T}{\partial t} \\ & = k_{\text{eff}} \frac{\partial^2 T}{\partial z^2} - \rho_{\text{gas}} C_{p\text{-gas}} \cdot \frac{\partial(u_z T)}{\partial z} - \rho_{\text{bulk}} \Delta H \frac{\partial q}{\partial t} \end{aligned} \quad (2)$$

The momentum of gas balance in the adsorber is expressed as follows:

$$\rho_{\text{gas}} \frac{\partial u}{\partial t} = \mu_{\text{gas}} \cdot \frac{\partial^2 u}{\partial z^2} - u_i \frac{\partial(u \rho_{\text{gas}})}{\partial z} - u \frac{\partial \rho_{\text{gas}}}{\partial t} - \frac{\partial P}{\partial z} \quad (3)$$

The material balance system in the adsorbent particle is expressed as follows:

$$\frac{\partial q}{\partial t} = D_{\text{pore},i} \left(\frac{\partial^2 q}{\partial r^2} + \frac{2}{r} \frac{\partial q}{\partial r} \right) \quad (4)$$

Initial conditions in calculation.

The gas density and concentration in the adsorber are expressed as follows:

$$\begin{aligned} P(z_k) &= P_{\text{initial}}, \quad y_i(z_k) = y_{\text{initial}} \\ \rho_i(z_k) &= \frac{P(z_k) \cdot y_i(z_k)}{M_i \cdot T(z_k) \cdot R_g} \end{aligned} \quad (5)$$

The gas velocity and temperature in the adsorber are expressed as follows:

$$u(z_k) = u_{\text{initial}}, \quad T(z_k) = T_{\text{initial}} \quad (6)$$

The amount of CO₂ in the adsorbent particle is expressed as follows:

$$q(P_{\text{CO}_2}) = q_{\text{initial}}(P_{\text{CO}_2}) \quad (7)$$

Boundary conditions.

1) Inlet of adsorber.

The gas density and concentration in the adsorber are expressed as follows:

$$\begin{aligned} P(z_0) &= P_{\text{ads}}, \quad y_i(z_0) = y_{i,\text{ads}} \\ \rho_i(z_0) &= \frac{P(z_0) \cdot y_i(z_0)}{M_i \cdot T(z_0) \cdot R_g} \end{aligned} \quad (8)$$

2) Outlet of adsorber.

a) Adsorption and Rinse step.

The gas density and concentration in the adsorber are expressed as follows:

$$\frac{\partial P(z_{k+1})}{\partial z} = 0, \quad \frac{\partial y_i(z_{k+1})}{\partial z} = 0 \quad (9)$$

The gas velocity and temperature in the adsorber are expressed as follows:

$$\frac{\partial u(z_{k+1})}{\partial z} = 0, \quad \frac{\partial T(z_{k+1})}{\partial z} = 0 \quad (10)$$

b) Desorption step.

The gas density and concentration in the adsorber are expressed as follows:

$$p(z_{k+1}) = P_{\text{back}}, \quad \frac{\partial y_i(z_{k+1})}{\partial z} = 0 \quad (11)$$

The gas velocity and temperature in the adsorber are expressed as follows:

$$u(z_{k+1}) = -u(z_k), \quad \frac{\partial T(z_{k+1})}{\partial z} = 0 \quad (12)$$

3) Surface of adsorbent particle.

The amount of CO₂ adsorption on the surface of the adsorbent particle is expressed as follows:

$$q_i(z_k, r_{\text{Ads},l+1}) = f_{q_i}(z_k, P_i) \quad (13)$$

4) Center of adsorbent particle.

The amount of CO₂ adsorption at the center of the adsorbent is expressed as follows:

$$\frac{\partial q_i(z_k, r_{\text{Ads},0})}{\partial r_{\text{Ads}}} = 0 \quad (14)$$

Subjunctive conditions.

- The effect of gravity is ignored.
- The interaction of each component in the adsorbent pore is ignored.
- Two-component system (CO₂-N₂).
- The density, heat capacity, and viscosity of each component are constant values.
- The momentum change is not affected by the adsorbent.

The coefficient for each transport phenomenon considered in the analysis model was obtained from previous studies [5] [6] [7]. The amount of the equilibrium CO₂ adsorption, adsorption heat, heat capacity, adsorbent density, and thermal conductivity of the adsorbent packed beds were experimentally determined. The coefficient values obtained from the numerical analysis are summarized in **Table 3**.

3. Analysis Results and Discussion

3.1. Consistency of Experimental and Simulation Results

The consistency of the experimental result obtained for the adsorption tower of ASCOA-3 was investigated with consideration to the developed analysis model described in the previous section. The analysis conditions are listed in **Table 4**. The actual gas exhausted by a steel process was introduced through an experiment, and the CO₂ density of the gas exiting the adsorption tower was measured.

When the adsorption tower reached the adhesion balance, the exit density reached the entrance density. To confirm the consistency of the analysis model, the breakthrough time of the CO₂ gas was estimated. The ratio of CO₂ breakthrough calculated the density of the CO₂ gas concentration at the exit as 1.0, which is equivalent to the CO₂ gas concentration at the entrance. The changes of the exit CO₂ density in the experimental and analysis results are shown in **Figure 2**. The CO₂ was mixed into the supply gas at 0 s. The adhesion of CO₂ progressed throughout the experiment, and breakthrough began at 830 s. It was found that the ratio of CO₂ breakthrough of 90% was reached in 1000 s. The breakthrough began at 810 s according to the calculation result obtained by the analysis model, and the ratio of CO₂ breakthrough exceeded 90% at 900 s. The CO₂ density changes in the adsorption tower and the aging of the absorbed amount are shown in **Figure 3** and **Figure 4**. The CO₂ and time course flow in the adsorption tower were higher compared with the analysis result. Additionally, it was found that the wear moved forward. The adhesion balance was mostly reached in the bed, as indicated by the time when the CO₂ breakthrough began. Therefore, the actual phenomenon was accurately expressed by the analysis model.

Table 3. List of coefficients in calculation.

	Symbol	Value	Reference
Langmuir Constant	A	0.29×10^{-3}	experiment
Equilibrium adsorption amount	q_{∞}	0.265	experiment
Packed bed in CO ₂ diffusion coefficient	D_{CO_2}	1.39×10^{-5}	M.F.Edwards (1968)
Pores in diffusion coefficient	D_{ads}	3.4×10^{-10}	Hirano, S. (2008)
Adsorption heat	ΔH_{ads}	996.6	experiment
Effective thermal conductivity of packed bed	k_{eff}	0.18	experiment
Specific adsorbent heat	Cp_{Ads}	1.13	experiment
Density of adsorbent	ρ_{Ads}	1940	experiment
Density of adsorbent packed bed	ρ_{beds}	684	experiment
Porosity of adsorbent packed beds	ε	0.566	experiment

Table 4. Conditions for adsorption breakthrough test and PSA cycle operation.

		Breakthrough	PSA cycle step		
			Adsorption	Rinse	Desorption
Gas flow rate	[Nm ³ /h]	100	478.9	-	-35.63
Operation total pressure	[kPa]	200.0	134.3	101.3	10
CO ₂ partial pressure	[kPa]	22.62	22.62	91.17	9.12
Duration	[s]	1400	150	50	100

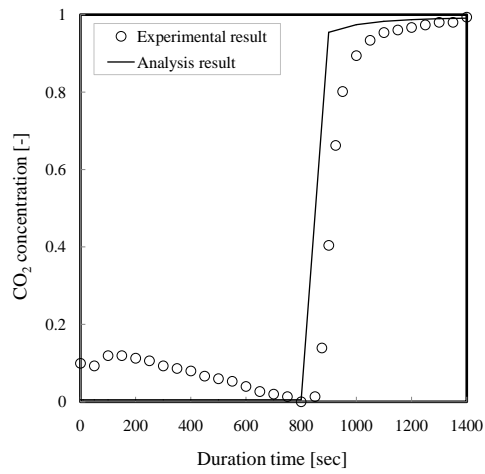


Figure 2. Comparisons between experimental and calculated CO₂ concentration in breakthrough test.

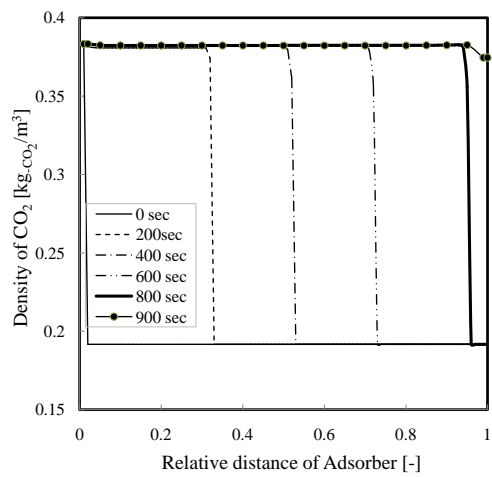


Figure 3. Temporal change in CO₂ concentration in adsorber over time in breakthrough test.

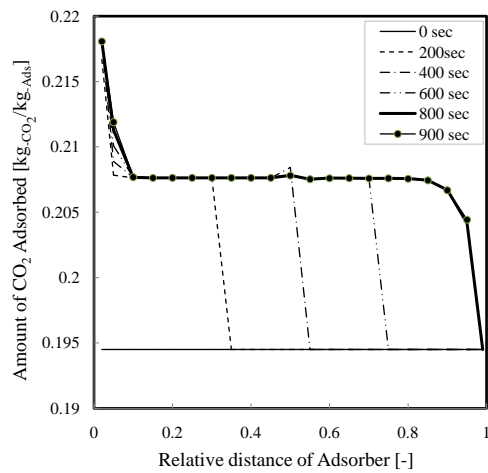


Figure 4. Temporal change in CO₂ adsorption amount in adsorber over time in breakthrough test.

3.2. Transport Phenomena in Adsorber

The adsorption under elevated pressure obtained by the analysis model, the washing, and the phenomena in the tower caused by the decompression attachment and removal process were considered. The driving conditions in each process are listed in **Table 4**. The pressure was boosted and 111.3 kPa were supplied to the gas washing process after adsorption under elevated pressure was provided by the decompression and desorption process. Therefore, the partial CO₂ pressure caused by the decompression attachment and removal process was equal to that of the washing process, and the flow rate was determined for the introduced gas differential-pressure at the tower entrance. The CO₂ pressure change and pick-up rate of 0.01 - 0.99 for each process at the Ainai location are presented in **Figure 5** and **Figure 6**. The time of 0 s was set for the decompression attachment and removal processes to complete 10 kPa. The dependence of CO₂ on the tower inflow by the adsorption in the elevated pressure process was higher than that in the analysis result, and the pressure increased. Subsequently, the pick-up rate reached the adhesion balance in 10 s at the tower entrance, and the CO₂ that was not absorbed performed advection at the lower part of the tower. From this point, there was almost no CO₂ inflow pressure and adhesion at the lower part of the tower (0.8 - 1.0) at 150 s during the adsorption at the end of the elevated pressure process, and it was found that CO₂ outflow to the exterior of the tower had not occurred. In the washing process, the pressure exhibited large fluctuations in the early stage under the influence of adhesion. At the end of the washing process, the adhesion advanced to the central part of the tower at 0.5 in 200 s. The pressure rapidly decreased in the decompression attachment and removal process, and the attachment and removal progressed. The pick-up rate also provided a good indication for the progress of the attachment and removal process. However, during the decompression attachment and removal process, the absorbed amount increased at the lower part of the tower. The reasons for this are as follows: CO₂ gas was introduced by the adsorption under elevated pressure; advection from the washing process occurred at the lower part of the tower; CO₂ adhered to the lower part of the tower. Thus, the CO₂ migration phenomena induced by each process are elucidated.

The aging changes for the N₂ density in the adsorption tower are shown in **Figure 7**. The adsorption under elevated pressure shows that the N₂ density increased over time at the adsorption tower entrance by the introduction of pressurized gas. Moreover, it was found that, during the washing process, the N₂ density at the exit, which is the lower part of the tower, was higher than that at the entrance. The N₂ that entered the tower with the introduction of CO₂ is a washing gas that spreads the advection throughout the lower part of the tower and then flows out through the tower exit. The N₂ amount that remains in the tower after the washing process is sufficiently smaller compared with the N₂ amount that remains after the process of adsorption under elevated pressure. Therefore, the N₂ amount left by the process of decompression attachment and removal is small, and CO₂ gas with high purity can be collected.

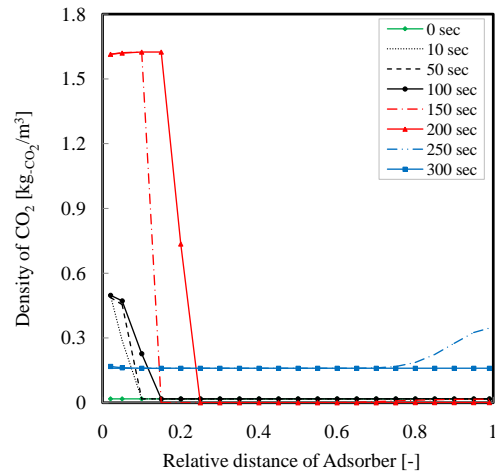


Figure 5. Temporal change of CO₂ concentration in adsorber with time in PSA cycle.

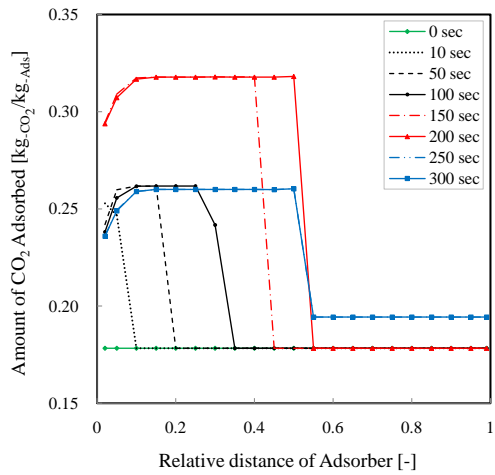


Figure 6. Temporal change of CO₂ adsorption amount in adsorber with time in PSA cycle.

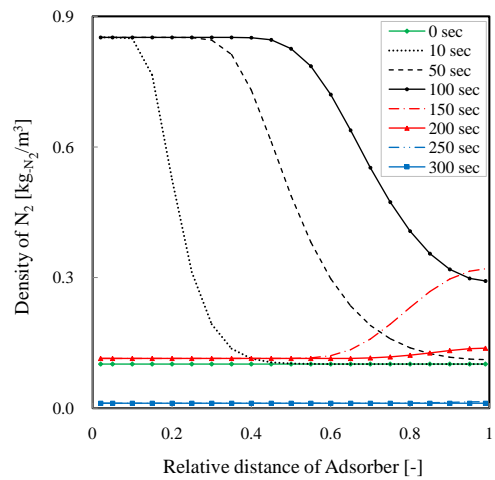


Figure 7. Temporal change of N₂ concentration in adsorber with time in PSA cycle.

The filling layer temperature in the adsorption tower was considered. The temperature at each filling layer location is indicated by the aging changes in **Figure 8**. In this process, the larger temperature difference began to change, but this influenced the adsorption and desorption heat. Compared with the tower entrance, the temperature in the tower increased more gradually with the progress of the adhesion caused by the adsorption in the elevated pressure process. Additionally, the adhesion progressed by the introduction of CO₂ gas in the washing process, and the temperature increased. At this time, the CO₂ adhesion caused by the high pressure was completed at location 0.15 in the tower. The temperature decreased to the adhesion heat caused by the heat transfer and advection to the lower part of the tower. Therefore, the temperature decreased at the end of the washing process. Subsequently, attachment and removal were performed in the decompression attachment and removal process, and the temperature decreased simultaneously. The time interval required for the temperature to change by 12 K at most, even if sufficient time is provided, was investigated. The adsorption and desorption heat calculated from the absorption isotherm obtained in this analysis was sufficiently small, compared with the adhesion heat induced by other adhesion pills and adhesion matter, because the adhesion pill considered in this study was combined with CO₂. Based on the absorption isotherm, the dependence of the absorbed amount is also small, and it is assumed that each fixed number does not depend on temperature. In this analysis, the temperature change did not influence the driving of the adsorption tower, and it was assumed that it is possible to drive while maintaining satisfactory performance.

The flow distribution at each location of the adsorption tower is shown in **Figure 9**. The flow rate that existed throughout is shown in **Figure 10**. Compared with the flow distribution, the adsorption exhibited significant fluctuations in the elevated pressure, washing, and decompression attachment and removal processes at the adsorption tower entrance. Notably, the adsorption under the elevated pressure process was 0.12 m/s in 100 s and 0.12 m/s by 0.03 m/s; the decompression attachment and removal process occurred at 300 s; the washing process occurred at 200 s. For the process to change, more flow distribution is caused by the advection of gas, and the phenomena of adsorption, desorption, and decompression occurs. Because it was put in the flow rate, it decompressed to the adsorption under the elevated pressure in the attachment and removal process. The absolute value was small. Additionally, N₂ existed because it accompanied a substantial amount of CO₂ in the gas collected by the decompression attachment and removal process and with adsorption under elevated pressure. The momentum that formed in the adsorption under the elevated pressure process spread throughout the adsorption at the lower part of the tower during the washing process, and CO₂ and N₂ flowed out. In the decompression attachment and removal process, the current velocity was reversed around the entrance to allow the current to be pulled in by the pulsometer through the adsorption tower entrance. However, the momentum that remained after the washing process performed advection at the lower part of the tower. Therefore,

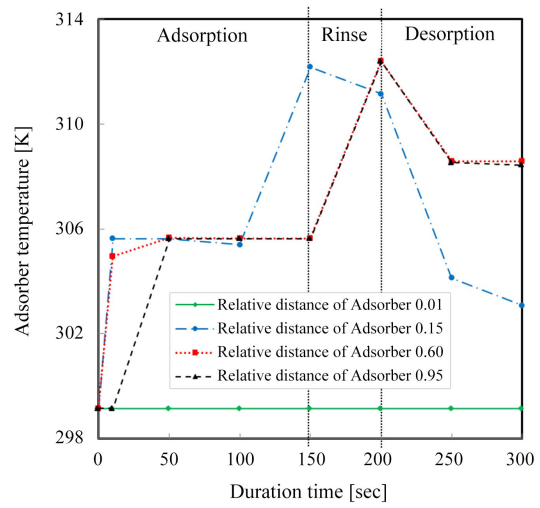


Figure 8. Temporal change of temperature in adsorber with time in PSA cycle.

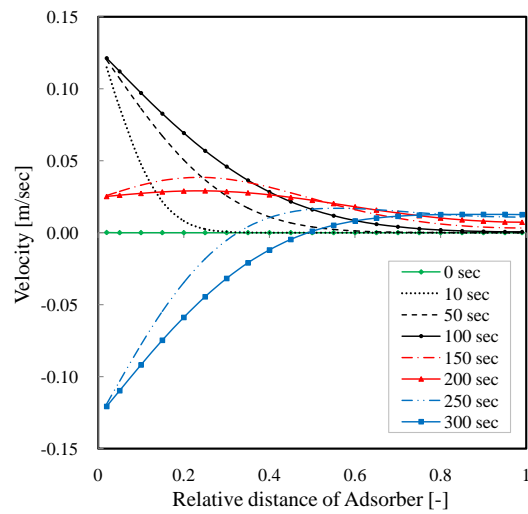


Figure 9. Temporal change of velocity in adsorber with time in PSA cycle.

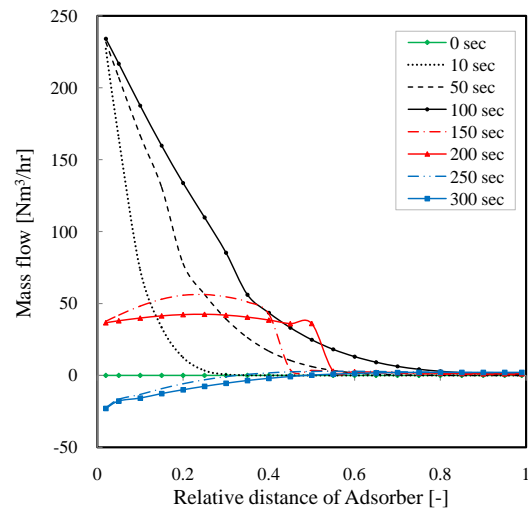


Figure 10. Temporal change of mass flow in adsorber with time in PSA cycle.

in the decompression attachment and removal process, CO₂ was pulled in by the pulsometer and collected at the entrance of the upper part of the tower. At the lower part of the tower, N₂ and CO₂ fluid flow occurred at the exit.

3.3. CO₂ Concentration and Recovery Ratio

With regard to the CO₂ density and CO₂ collection rate, the electric power of the pulsometer yielded twice as much and the CO₂ with the driving of the adsorption tower compared with that considered in the analysis. This result was compared with the experimental result obtained for the adsorption tower by the bench scale experiment. The analysis results and experimental results are presented in **Table 5**. The CO₂ density is the average CO₂ density of the gas obtained during the decompression attachment and removal process. The CO₂ collection rate is the percentage of CO₂ collected in the decompression attachment and removal process to the CO₂ amount introduced in the adsorption process under elevated pressure. The pulsometer power can be used to calculate the electric power of the pump from the suction pressure and flow rate used in the decompression attachment and removal process. The amount of collected CO₂, which is later introduced to the driving through a set of adsorption towers, was standardized in one day.

Value equal to the experimental results were mostly obtained in the analysis results. However, the CO₂ density was approximately 90% higher than the analysis result. In the adsorption under elevated pressure and washing processes, the CO₂ did not flow through the tower exit because the remaining N₂ was collected in the pulsometer along with CO₂ during the decompression attachment and removal process. It was found that 24% of the CO₂ that was introduced by adsorption under elevated pressure while driving in the decompression attachment and removal process of 10 kPa could not be collected at the current rate of collection. Compared with the analysis result, this is more depended on the outflow to adhesion and outside of the tower caused by the lower part of the tower in the decompression attachment and removal process. The pulsometer power and C, which will later be present in industrial applications, need improvement of the O twice yield. It is necessary to consider that the quantity of the introduced gas flow, and the diameter and height of the adsorption tower, influence the time of each process in the driving of the PSA cycle. With the model used in the analysis, the collected amount increased because 24% of CO₂ was not collected. From this point onward, the design factor for scaling up, by which we assume that it is possible to increase the throughput, and the sensitivity analysis results were obtained.

Table 5. Accuracy validation for calculation model of PSA cycle.

	Experiment	Analysis	unit
CO ₂ concentration	91.0	93.4	%
CO ₂ recovery ratio	77.0	76.4	%
Pump powerconsumption for CO ₂ capture	186.0	196.7	kwh/ton _{CO2}
CO ₂ amount recovered	3.2	2.9	ton/day

4. Conclusions

This study carried out CO₂ separation with consideration to scaling up and developed a PSA method for CO₂ collection. A model was built for the income and expenditure system of the substance in the adsorption tower, and the heat, momentum, and migration in the tower were estimated by numerical analysis. The physical properties of the analysis model were obtained by experiment, and the consistency between the experimental result, which was obtained using a bench-scale adsorption tower, and the developed analysis model was investigated. The following conclusions were drawn from this study:

1) The migration phenomenon of the substance in the tower, the energy, and the momentum were expressed in the C programming language, and the analysis model of a possible PSA route was established. The CO₂ density at the adsorption tower, absorbed amount, temperature, and flow distribution in the PSA driving process were investigated, and the influence on the CO₂ collection was confirmed to be higher compared with that in the analysis result.

2) The breakthrough opening time in the CO₂ adsorption breakthrough test was 830 s, the CO₂ density in the tower was balanced, and breakthrough was initiated. This result is identical to the opening time in the bench scale experiment.

3) With a CO₂ concentration of 93.4% in the captured gas and a CO₂ quantity of 2.9 ton/day, twice as much CO₂ was obtained from the density of CO₂ collected by PSA driving. This value is approximately equal to the value of the adsorption tower in the bench scale experiment. Additionally, this model can be useful as an analysis tool in future scale-up studies.

Conflicts of Interest

The authors declare no conflicts of interest regarding the publication of this paper.

References

- [1] Aaron, D. and Tsouris, C. (2005) Separation of CO₂ from Flue Gas: A Review. *Separation Science and Technology*, **40**, 1-3, 321-348. <https://doi.org/10.1081/SS-200042244>
- [2] Kodama, A., Seo, M., Miyashita, Y. and Osaka, Y. (2013) Separation of a Simulated Biogas Mixture (Methane-Carbon Dioxide-Water Vapor) by Pressure Swing Adsorption with SAPO-34. *Kagaku Kougaku Ronbunshu*, **39**, 503-507.
- [3] Choi, W., Kwon, T., Yeo, Y., Lee, H., Song, H. and Na, B. (2003) Optimal Operation of the Pressure Swing Adsorption (PSA) Process for CO₂ Recovery. *Korean Journal of Chemical Engineering*, **20**, 617-623. <https://doi.org/10.1007/BF02706897>
- [4] Anshul, A. and Lorenz, T.B. (2010) A Superstructure-Based Optimal Synthesis of PSA Cycles for Post-Combustion CO₂ Capture. *AIChE Journal*, **56**, 1813-1828. <https://doi.org/10.1002/aic.12107>
- [5] Hirano, S. (2008) The Effect of Macropore of Zeolite Adsorbents for Dynamic Adsorption Properties. *TOSOH Research & Technology Review*, **52**, 55-60. (In Japanese).

- [6] Yang, H., Xu, Z., Fan, M., Gupta, R., Slimane, R.B., Bland, A.E. and Wright, I. (2008) Progress in Carbon Dioxide Separation and Capture: A Review. *Journal of Environmental Sciences*, **20**, 14-27. [https://doi.org/10.1016/S1001-0742\(08\)60002-9](https://doi.org/10.1016/S1001-0742(08)60002-9)
- [7] Edwards, M.F. and Richardson, J.F. (1968) Gas Dispersion in Packed Beds. *Chemical Engineering Science*, **23**, 109-123. [https://doi.org/10.1016/0009-2509\(68\)87056-3](https://doi.org/10.1016/0009-2509(68)87056-3)

Nomenclature

A	=Langmuir constant	[kPa ⁻¹]
C_p	=heat capacity	[kJ·K ⁻¹]
D	=diffusion coefficient	[m ² ·s ⁻¹]
$f_{q_{CO_2}}$	=fraction of adsorption amount	[-]
I	=electrical current	[A]
ΔH	=adsorption heat	[kJ·kg ⁻¹]
k_{eff}	=effective thermal conductivity	[W·m ⁻¹ ·K ⁻¹]
M	=molecular weight	[kg·mol ⁻¹]
P	=pressure	[kPa]
q	=adsorption amount	[kg·CO ₂ ·kg ⁻¹ ·Ads]
q_∞	=equilibrium adsorption amount	[kg·CO ₂ ·kg ⁻¹ ·Ads]
R	=electrical resistance	[Ω]
R_g	=gas constant	[kJ·K ⁻¹ ·mol ⁻¹]
T	=temperature	[K]
t	=time	[s]
r	=particle diameter	[m]
u	=velocity	[m·s ⁻¹]
v	=pore volume	[m ³ ·kg ⁻¹]
y	=mole fraction	[-]
z	=length	[m]
ε	=porosity	[-]
ρ	=density	[kg·m ⁻³]
μ	=viscosity	[kPa·s]
<subscripts>		
0	=inlet	
Ads	=adsorbent	
ads	=adsorption	
ave	=average	
back	=desorption step	
bulk	=adsorbent packed beds	
CO ₂	=carbon dioxide	
gas	=gas fluid	
i	=component	
initial	=initial	
k	=repetition number (adsorber axial direction)	
l	=repetition number (particle center direction)	
pore	=adsorbent pore	
α	=true density of adsorbent	
β	= apparent adsorbent density	